Hierarchical Helical Order in the Twisted Growth of Plant Organs

Hirofumi Wada

Department of Physics, Ritsumeikan University, Kusatsu 525-8577, Shiga, Japan

(Received 28 April 2012; revised manuscript received 4 July 2012; published 19 September 2012)

The molecular and cellular basis of left-right asymmetry in plant morphogenesis is a fundamental issue in biology. A rapidly elongating root or hypocotyl of twisting mutants of *Arabidopsis thaliana* exhibits a helical growth with a handedness opposite to that of the underlying cortical microtubule arrays in epidermal cells. However, how such a hierarchical helical order emerges is currently unknown. We propose a model for investigating macroscopic chiral asymmetry in *Arabidopsis* mutants. Our elastic model suggests that the helical pattern observed is a direct consequence of the simultaneous presence of anisotropic growth and tilting of cortical microtubule arrays. We predict that the root helical pitch angle is a function of the microtubule helical angle and elastic moduli of the tissues. The proposed model is versatile and is potentially important for other biological systems ranging from protein fibrous structures to tree trunks.

DOI: 10.1103/PhysRevLett.109.128104 PACS numbers: 87.19.lx, 46.70.Hg, 87.19.R−

Helical growth is often found in plants with twining tendrils and spiral order of leaves, petals, or florets. For many years, the molecular and cellular basis of left-right asymmetry as well as the potential importance of this asymmetry in biological functions has been a fundamental issue in biological sciences. In general, plant shape and movement are the consequences of directional cell expansion resulting from force balance between turgor pressure and cell wall tension [1–4]. Therefore, the spatial distribution of wall microfibrils determines the polarity of cell expansion and the resulting morphogenesis. A recent experiment has shown that cortical microtubules serve as a cytoplasmic template for microfibril orientation [5], confirming that membrane-assisted cortical microtubules direct cellulose microfibril alignment [6,7].

The twisting mutants of *Arabidopsis thaliana* provide an ideal system for studying the relationship between microtubule organization and the chirality in organ growth (see Fig. 1) [8]. In wild-type plants, rapidly expanding axial organs such as roots and hypocotyls maintain straight expansion. The microtubule array of root cells is aligned transverse to the primary growth axis, and it appears as a stack of ringlike bundles. In contrast, the growth direction of the epidermal cell files in the twisting phenotype is continuously tilted either to the right or left (see Fig. 1), which involves an oblique microtubule array that shows helical ordering. Interestingly, a strong correlation has been experimentally established between chirality in organ growth and alignment of the helical microtubule array: right-handed helical growth mutants possess left-handed microtubule arrays, whereas left-handed mutants possess right-handed arrays [8–11]. This remarkably simple relationship implies an underlying mechanical basis of the macroscopic left-right asymmetry in *Arabidopsis* twisting mutants, which is, however, currently unknown. In a biological model proposed in Ref. [9], organ twisting has been attributed to differences in cell elongation between inner and outer layers, but the mechanism of chiral selection has not been explained by this model [8].

In this Letter, we present a linear elasticity theory to investigate the mechanical basis underlying the hierarchical helical order in *Arabidopsis* mutants. We propose a simplistic model that relies on the fundamental assumption that plant organ morphology is governed by mechanical stresses generated by helical growth at a single-cell level [12]. In particular, we consider that each epidermal cell exhibits helical growth because of the tilted alignment of wall microfibrils. At the organ level, however, an individual cell cannot rotate freely about its axis in order to maintain the structure of the organ. The elasticity and long-term plasticity of the organ enable the cell files to generate torsion about the root primary axis to partially relieve these growth-induced stresses. Consequently, the

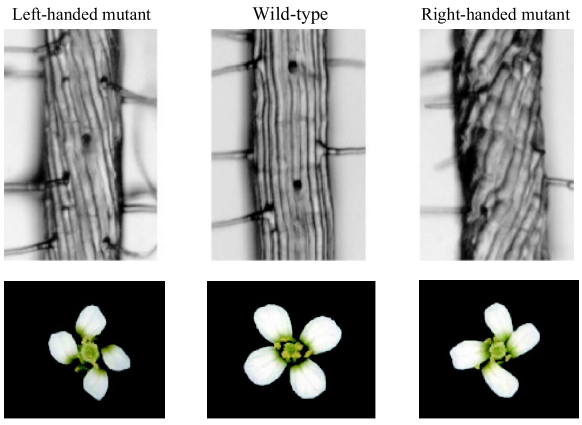

FIG. 1 (color online). Root epidermis and flower petals of *Arabidopsis thaliana*: wild-type (center), left-handed mutant (left panel), and right-handed mutant (right panel). Image courtesy Takashi Hashimoto.

helical growth at the single-cell level organizes the growth of the organ in one coherent direction owing to long-range elasticity. This scenario also provides a natural explanation for the well-established chiral relationship described above. Our calculations predict how the helical angle varies with the microtubule helical angle and the ratio of the elastic moduli of inner and outer cell layers.

Similar to other systems that exhibit helical growth, an elongating cylindrical rod generates twist when the growth direction is tilted from its primary axis [13,14]. We have not considered the possible residual stress that is generated during growth [15–17] and have focused only on the growth kinematics of epidermal cells. Given that the microtubules direct the alignment of the cellulose microfibrils, the growth direction of the cell wall is transverse to the microtubule array. In Fig. 2, the helical ribbon represents the cortical microtubule array, and the solid violet circles represent the trajectory of a labeled material point. When the microtubules align to form regular helices, the trajectory of the material point should also be a helical line with opposite handedness.

The growth of cells in *Arabidopsis* roots is highly anisotropic. Once the cells leave the cell division zone, no appreciable radial expansion occurs, and individual cell growth at a typical growth velocity $\sim \mu$m/ min is completed in a few hours [18]. We have thus modeled these cells as a cylindrical rod that grows in length but maintains a constant radius r_0. Because the elongation zone is much larger than the radius, we assume that spatially uniform growth occurs in the axial direction. By considering the manner in which a given point on the rod with coordinates (ρ, φ, s) is convected during a short period dt owing to growth, we can obtain the growth kinematic equations $\dot{\rho} = 0$, $\dot{\varphi} = (\sigma_1 - \sigma_2)(s/\rho)\sin\theta\cos\theta$, and $\dot{s} = (\sigma_1 \sin^2\theta + \sigma_2 \cos^2\theta)s$, where the dot represents the time derivative and σ_1 and σ_2 are the growth rates in the two principal directions (see Fig. 2). By solving these equations, we can determine the growth mode of a single epidermal cell as follows:

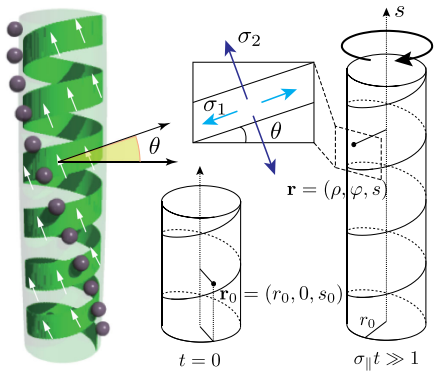

FIG. 2 (color online). Left: Helical growth of a single epidermal cell with a right-handed helical microtubule array. The violet points trace the left-handed twist during growth. Right: Geometry of the helical growth model described in the main text.

$$\rho = r_0, \tag{1}$$

$$\varphi(t) = \frac{\sigma_1 - \sigma_2}{\sigma_\parallel} \sin\theta\cos\theta \frac{s_0}{r_0}(e^{\sigma_\parallel t} - 1), \tag{2}$$

$$s(t) = s_0 e^{\sigma_\parallel t}, \tag{3}$$

where we have defined the axial growth rate $\sigma_\parallel = \sigma_1 \sin^2\theta + \sigma_2 \cos^2\theta$, which is a combination of the two growth rates. The arc length grows exponentially with time, and the cross section of the cylinder rotates with an angular velocity that increases with arc length.

For a short time regime characterized by $\sigma_\parallel t \ll 1$, we found the linear increase in rotating angle $\varphi(s_0, t) \approx (\sigma_1 - \sigma_2)t(s_0/r_0)\sin\theta\cos\theta$, which agrees with the result provided by Schulgasser and Wiztum without derivation [19]. They originally considered a spontaneous rotation of a cylindrical tube undergoing thermal expansion. Equation (2) is thus a generalization of their result to the one applicable to a growing elastic cylinder. An important result obtained from Eq. (2) is the kinematics over long time scales. For $\sigma_\parallel t \gg 1$, the rotation angle of the material (originally at s_0 at $t = 0$) with respect to that at $s = 0$ increases exponentially with time but linearly with s, i.e., $\varphi(s_0, t) \approx \tau_0 s_0 e^{\sigma_\parallel t} = \tau_0 s$. The growth-induced twist τ_0 is found to be uniform along the rod and is given by

$$\tau_0(\theta, \alpha) = -\frac{1}{r_0} \frac{\alpha \sin 2\theta}{1 + \alpha \cos 2\theta}, \tag{4}$$

which depends only on the microtubule helical angle θ and the ratio of the growth rates $\alpha = -(\sigma_1 - \sigma_2)/(\sigma_1 + \sigma_2)$. It should be noted that the same exponential growth model was previously used to describe the supercoiling instability of growing *Bacillus subtilis* fibers [20], where τ_0 denoted a certain constant parameter. Equation (4) helps elucidate how τ_0 depends on the growth rate and cell wall anisotropy and can be applied to a wide variety of growing biological filaments.

The thick inextensible epidermal cell layer sheathes relatively more compliant inner tissues [7]. We have thus modeled the entire organ as a composite elastic body consisting of the inner and outer cell layers (see Fig. 3). The outer layer is a parallel bundle of N identical rods with an intrinsic twist τ_0 and total length L. The center lines of rods, parameterized by their arc length s, are helices wrapped around a core cylinder of radius $R - r_0$, and we used a variational approach to determine their equilibrium shapes, assuming that these rods were closely packed. This approach is similar to those used in the study of the mechanics of n-plies, which are relevant to a wide class of engineering issues such as those experienced for textiles and wire ropes (e.g., Ref. [21] and references therein). The n-ply issue related to the central core cylinder has recently been analyzed by appropriately taking the ply geometry into account but for a prescribed and constant twist of the

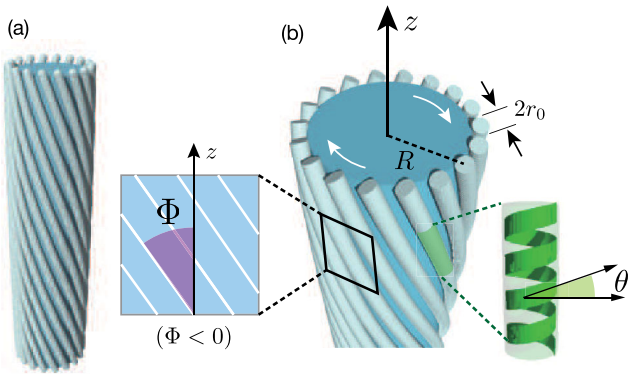

FIG. 3 (color online). (a) Schematic representation of the root or hypocotyl organ. (b) Composite elastic model for a cylindrical organ with constant radius R. The inner and outer layers share growth-induced stress via tissue tension. The inter-rod distances are somewhat overdrawn.

core cylinder [22]. In the current analysis, the core twist is induced by the skewing of the outer rods and is determined self-consistently so that it minimizes the elastic energy of the entire system.

The center line of the n-th rod has a uniform helical shape with a fixed (known) radius R and is given by $\mathbf{R}_n(s) = [R\cos\psi_n(s), R\sin\psi_n(s), s\cos\Phi]$, where $\psi_n(s) = (\sin\Phi/R)s + 2\pi n/N$ is the equatorial angle in a plane perpendicular to the long axis of the root growth [23]. The pitch angle Φ is shown in Fig. 3(b) and has plus and minus signs for right- and left-handed helices, respectively. Taking into account the growth-induced twist given by Eq. (4), the elastic deformation energy of the collection of N-rods is expressed as $E_{\text{out}} = N\int_0^L ds[(A/2)\kappa^2 + (C/2)(\omega - \tau_0)^2]$, where κ is the curvature, ω is the twist density, and A and C are the effective bending and twisting moduli, respectively [21,24]. Because the rigidity of an epidermal cell dominantly arises from its thin tubelike cell wall with a thickness of h, we use $A = \pi E r_0^3 h$ and $C = 2\pi\mu_E r_0^3 h$, which are valid for $h/r_0 \ll 1$ [24,25]. E and μ_E are the Young's modulus and shear modulus of the cell wall, respectively, and typically, $E \sim$ GPa [4].

We adopted a standard assumption in which the growth of the organ is slow enough as compared to the typical time required to attain mechanical equilibrium [17,26]. Consequently, we considered a quasistatic limit at which the state of the system can be determined by minimizing the elastic deformation energy of the root organ E under the material parameters given by the growth process. Over a much longer time scale, these parameters change gradually, leading to so-called plastic deformation (morphoelasticity) [16,27].

By performing the standard frame transformation, we can express the twist density in terms of the center line geometry and the axial spinning degree of freedom, which leads to the expression $\omega = (d\varphi/ds) + \tau$. Here, τ is the geometric torsion and $d\varphi/ds$ is termed the excess twist [28]. If a rod is free to rotate about its axis, the minimum energy configuration is a straight rod with a uniform axial twist, i.e., $\varphi(s) = \tau_0 s$ and $\kappa = \tau = 0$, which is the configuration required according to the kinematics given by Eq. (3). In reality, however, the cells are glued in order to maintain the structure of the entire organ, thus preventing an individual cell from rotating about its long axis. We can treat this organ structure as another geometric constraint given by

$$d\varphi/ds = 0 \quad \text{for} \quad 0 \le s \le L. \tag{5}$$

For a uniform helical configuration, the constant curvature and torsion are expressed as $\kappa = \sin^2\Phi/R$ and $\tau = \sin\Phi\cos\Phi/R$, respectively [24,28]. Using the constraint given by Eq. (5), the elastic deformation energy of the outer layer is $E_{\text{out}} = N\int_0^L e_{\text{out}}(\Phi)ds$, where $e_{\text{out}}(\Phi) = A/2(\sin^4\Phi/R^2) + C/2(\sin\Phi\cos\Phi/R - \tau_0)^2$.

Growth-induced stress can also be transmitted to the inner cortex cell layer via extracellular matrices. This load sharing is termed tissue tension [7,29,30]. See Fig. 3(b). Thus, the total elastic energy of the organ is the sum of the inner and outer energies, i.e., $E = E_{\text{in}} + E_{\text{out}}$. We considered the inner cortex tissues as a uniform elastic medium with an effective shear modulus μ_C. As this medium contains an almost fluid phase ($\sim 75\%$ [4]), we expect to obtain $\mu_C/\mu_E \ll 1$. Further, the cortex cells of etiolated hypocotyls are experimentally observed to possess microtubule arrays of mixed polarities, without showing any defined handedness [8,9]. Therefore, we neglected the buildup of any growth-induced stress by the cortex cell itself. The elastic energy of the cortex layer thus becomes equivalent to that of a uniformly twisted rod with radius $R - r_0$ and torsion $\Omega = \tan\Phi/(R - r_0)$, providing $E_{\text{in}} = (\pi/4)\mu_C(R - r_0)^2\int_0^L \sin\Phi\tan\Phi ds$. Note that the close-packing geometry imposes the constraint $2\pi\cos\Phi/N = 2r_0/R$, suggesting that the number of rods varies with Φ according to $N = N_0\cos\Phi$, where $N_0 = \pi R/r_0$. Furthermore, this simple relation holds true only when $N \gg 1$ and is valid for *Arabidopsis* roots (typically $N =$ 30–40 [8]). Therefore, the total elastic energy is now written in the form $E = E_{\text{in}} + E_{\text{out}} = N_0\int_0^L e(\Phi)ds$, where $e(\Phi) = e_{\text{out}}(\Phi)\cos\Phi + (\pi\mu_C/4N_0)(R - r_0)^2\sin\Phi\tan\Phi$. The equilibrium pitch angle $\Phi(\theta, \alpha)$ is determined by the equation $de(\Phi)/d\Phi = 0$, which yields

$$\begin{aligned} 0 = {} & (1+\nu)\sin^2\Phi(4\cos^2\Phi - \sin^2\Phi) + \gamma(2 + \tan^2\Phi) \\ & + (2\cos 2\Phi\cot\Phi - \tfrac{1}{2}\sin 2\Phi + \tau_0 R)(\tfrac{1}{2}\sin 2\Phi - \tau_0 R), \end{aligned} \tag{6}$$

where $\nu = A/C - 1$ is the Poisson's ratio and $\gamma = \frac{\pi\mu_C R^4}{2N_0 C}$. Substituting the expressions for C and N_0 given above into γ, we find $\gamma = (r_0/4\pi h)(R/r_0)^3(1 - r_0/R)^2(\mu_C/\mu_E)$. For sufficiently small Φ, the approximate solution of Eq. (6) is found to be

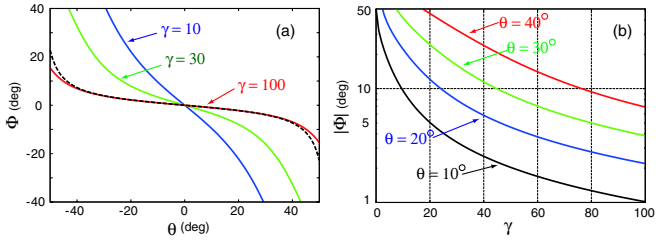

FIG. 4 (color online). Numerical solutions of Eq. (6): Φ as a function of (a) microtubule helical angle θ and (b) coupling strength γ (semilog scale). The relevant parameters have been taken from *Arabidopsis* data, and $R_0/r_0 = 10$, $\alpha = 1$, and $\nu = 0.5$. The dashed line represents the linearized analytic solution given by Eq. (7) for (a) $\gamma = 100$.

$$\Phi \simeq \frac{R\tau_0(\theta, \alpha)}{1 + \gamma - \frac{1}{2}R^2\tau_0^2(\theta, \alpha)}. \tag{7}$$

For purely unidirectional growth, i.e., $\sigma_1 = 0$, we obtain $\Phi = -(R/r_0)\tan\theta/(1 + \gamma - R^2/(2r_0^2)\tan^2\theta)$. The equations (4) and (7) constitute the main result of this paper. Several conclusions can be drawn from Eq. (7). First, when either the growth is isotropic, i.e., $\alpha = 0$, or when the microtubule array does not tilt, i.e., $\theta = 0$, we obtain $\Phi = 0$. Thus, the helical growth of *Arabidopsis* mutants is a direct consequence of the simultaneous presence of the helical microtubule array and anisotropic growth. Second, because $0 \leq \alpha \leq 1$, the handedness of the microtubule helices is always *opposite* to that of the helical growth of the organ, which is entirely consistent with the detailed observations. Finally, the ratio of the inner or outer elastic moduli, γ, is a key parameter that governs the magnitude of Φ, which was not addressed in the previous model [9]. Interestingly, the ratio of inner to outer (or core to shell) moduli has been suggested as one of the critical parameters that determine the skin patterns of other plants such as certain fruit and vegetable plants [31].

The numerical solutions of Eq. (6) are plotted in Fig. 4 as functions of the microtubule array angle θ and the coupling strength γ. For certain values of γ, Eq. (6) allows multiple solutions; therefore, the lowest energy solution is plotted in Fig. 4 [32]. The experimental parameters are estimated as follows: From the images shown in Refs. [9,33,34], we see $N_0 \sim 30$, thus $R/r_0 \sim N_0/\pi \sim 10$. Because many biological materials are nearly incompressible, we used the Poisson's ratio of the cell wall $\nu = 0.5$ [26]. Radial and circumferential stretching are not observed during the growth of individual epidermal cells, except during the initial growth stage [18]. Therefore, we set $\sigma_1 = 0$ (and thus $\alpha = 1$). The cell wall of an individual epidermal cell is generally very thin, but to our knowledge, no precise value is available for its thickness [35]. Images of chemically stained dead cells [33] and live cell images from phase contrast microscopy [34] suggest that the cell wall of these cells is very thin and its value is less than 10% of its radius. We therefore assumed $h/r_0 \sim 0.05$, which leads to $\gamma \sim 1300 \times \mu_C/\mu_E$. Because μ_C/μ_E is unknown, we plotted the values of γ and Φ in Fig. 4(b) to observe how the root angle Φ varies with γ. Through systematic experimental measurements, the magnitude of Φ was found to be 5°–10° with $\theta = 30°$–40° for left-handed helical growth mutants, i.e., lefty [10], whereas the magnitude of Φ was found to be 10°–20° with $\theta = 20°$–30° for right-handed helical mutants, i.e., spiral [9]. From Fig. 4, we obtained $\gamma \sim 80$ or $\mu_C/\mu_E \sim 0.06$ for *lefty* mutants and $\gamma \sim 25$ or $\mu_C/\mu_E \sim 0.02$ for *spiral* mutants. The predicted difference in the shear moduli between two layers is substantial and can be investigated in future experiments.

The helical growth of an epidermal cell in a cell suspension has been directly observed in a recent experiment [12], which provides a solid experimental ground for our modeling assumption. The mechanism underlying the establishment of microtubule helical arrangement is being explored by other microscopic modeling approaches also [36–38]. We note that the present analysis lacks a few key features necessary for a realistic description of plant tissue growth, such as the effects of turgor pressure, residual stress, and wall reinforcements. Because soft tissues often undergo large deformations in response to physiological loading, their physical properties should be modeled within the theory of finite elasticity in future extensions of this study, as done in Refs. [30,39]. Nevertheless, the proposed model can explain how the microscopic chirality determines the macroscopic chirality affected only by the long-range elastic interactions. This information will be potentially useful in understanding other superhelical structures over various biological scales, ranging from filamentous protein assemblies to stems, arteries, and tree trunks.

I am grateful to Professor Hashimoto (Nara Institute of Science and Technology) for sharing the image shown in Fig. 1 and for valuable discussions. Financial support from MEXT-Japan (Grant in Aid, No. 22740274) is acknowledged.

[1] D'Arcy W. Thompson, *On Growth and Form: The Complete Revised Edition* (Dover, New York, 1992).
[2] N. Kamiya, M. Tazawa, and T. Takada, Protoplasma **57**, 501 (1963).
[3] J. M. Skotheim and L. Mahadevan, Science **308**, 1308 (2005).
[4] J. Dumais and Y. Forterre, Annu. Rev. Fluid Mech. **44**, 453 (2012).
[5] A. R. Paredez, C. R. Somerville, and D. W. Ehrhardt, Science **312**, 1491 (2006).
[6] B. E. S. Gunning and M. W. Steer, *Plant Cell Biology: Structure and Function* (Jones and Bertlett Pubishers, Burlington, Massachusetts, 1996).
[7] T. I. Baskin, Annu. Rev. Cell Dev. Biol. **21**, 203 (2005).
[8] T. Ishida, S. Thitamadee, and T. Hashimoto, J. Plant Res. **120**, 61 (2007).

[9] I. Furutani, Y. Watanabe, R. Prieto, M. Masukawa, K. Suzuki, K. Naoi, S. Thitamadee, T. Shikanai, and T. Hashimoto, Development **127**, 4443 (2000).
[10] S. Thitamadee, K. Tuchihara, and T. Hashimoto, Nature (London) **417**, 193 (2002).
[11] T. Ishida, Y. Kaneko, M. Iwano, and T. Hashimoto, Proc. Natl. Acad. Sci. U.S.A. **104**, 8544 (2007).
[12] H. Buschmann, M. Hauptmann, D. Niessing, C. W. Lloyd, and A. R. Schäffner, Plant Cell **21**, 2090 (2009).
[13] P. A. Roelofsen, Adv. Bot. Res. **2**, 69 (1966).
[14] A. Goriely and M. Tabor, Phys. Rev. Lett. **106**, 138103 (2011).
[15] E. K. Rodriguez, A. Hoger, and A. D. McCulloch, J. Biomech. **27**, 455 (1994).
[16] A. Goriely, M. Robertson-Tessi, M. Tabor, and R. Vandiver, in *Mathematical Modeling of Biosystems*, edited by R. P. Mondaini and P. M. Pardalos (Springer-Verlag, Berlin, 2008), pp. 1–44.
[17] J. Dervaux and M. Ben Amar, Phys. Rev. Lett. **101**, 068101 (2008).
[18] K. Sugimoto, R. E. Williamson, and G. O. Wasteneys, Plant Physiol. **124**, 1493 (2000).
[19] K. Schulgasser and A. Witztum, J. Theor. Biol. **230**, 281 (2004).
[20] C. W. Wolgemuth, R. E. Goldstein, and T. R. Powers, Physica (Amsterdam) **190D**, 266 (2004).
[21] S. Neukirch and G. H. M. van der Heijden, J. Elast. **69**, 41 (2002).
[22] T. Morimoto and H. Iizuka, Compos. Struct. **94**, 1575 (2012).
[23] S. Neukirch, A. Goriely, and A. C. Hausrath, Phys. Rev. Lett. **100**, 038105 (2008).
[24] B. Audoly and Y. Pomeau, *Elasticity and Geometry* (Oxford University Press, New York, 2010).
[25] L. D. Landau and Lifshitz, *Theory of Elasticity* (Butterworth Heinemann, Boston, 1986).
[26] A. Boudaoud, Phys. Rev. Lett. **91**, 018104 (2003).
[27] R. E. Goldstein and A. Goriely, Phys. Rev. E **74**, 010901 (R) (2006).
[28] A. E. H. Love, *A Treatise on the Mathematical Theory of Elasticity* (Dover, New York, 1944).
[29] Z. Hejnowicz and A. Sievers, J. Exp. Bot. **47**, 519 (1996).
[30] R. Vandiver and A. Goriely, Phil. Trans. R. Soc. A **367**, 3607 (2009).
[31] J. Yin, Z. Cao, C. Li, I. Sheinman, and X. Chen, Proc. Natl. Acad. Sci. U.S.A. **105**, 19132 (2008).
[32] The solution to Eq. (6) is generally unique for the parameters relevant to *Arabidopsis*. Two other solutions can appear for small γ and large θ, with higher elastic energies. One is energetically unstable, the other is locally stable with its chirality opposite to that of the lowest energy solution. More details will be reported elsewhere (H. Wada to be published).
[33] L. Dolan, K. Janmaat, V. Willemsen, P. Linstead, S. Poethig, K. Roberts, and B. Scheres, Development **119**, 71 (1993).
[34] J. E. Malamy and P. N. Benfey, Development **124**, 33 (1997).
[35] T. Hashimoto (private communication).
[36] E. C. Eren, R. Dixit, and N. Gautam, Mol. Biol. Cell **21**, 2674 (2010).
[37] R. J. Hawkins, S. H. Tindemans, and B. M. Mulder, Phys. Rev. E **82**, 011911 (2010).
[38] C. L. Henley, arXiv:1112.2317v1 [J. Stat. Phys. (to be published)].
[39] A. Goriely, D. E. Moulton, and R. Vandiver, Europhys. Lett. **91**, 18001 (2010).